SIMULATION OF NOISE WITHIN BOTDA AND COTDR SYSTEMS TO STUDY THE IMPACT ON DYNAMIC SENSING

Adam Funnell, Xiaomin Xu, Jize Yan*, Kenichi Soga

Department of Engineering

University of Cambridge

Cambridge CB2 1PZ, United Kingdom

Email: *yanjize@gmail.com

Submitted: June 22, 2015 ***Accepted: July 16, 2015*** ***Published: Sep. 1, 2015***

Abstract- Real-time structural health monitoring requires dynamic sensing of distributed strain and temperature. Brillouin Optical Time Domain Analysis (BOTDA) and Rayleigh Coherent Optical Time Domain Reflectometry (COTDR) are promising candidates to achieve dynamic sensing. A noise model with specific parametric simulation of independent laser and detector noise sources has been developed. Although ensemble averaging significantly enhances the signal-to-noise ratio (SNR) in both systems, its time-consuming accumulation procedure prevents dynamic sensing. The sequence of averaging in the signal processing workflow varies the SNR for both systems. The system components should be optimized to reduce averaging times and achieve the required system specifications, including dynamic sensing.

Index terms*: dynamic sensing, noise simulation, BOTDA, COTDR, laser fluctuation, detection, averaging*

I. INTRODUCTION

Distributed fibre optic sensing (DFOS) systems use the interactions between light and an optical fibre confining it to infer details about the strain, temperature and vibration along the fibre with a consistent accuracy [1-4]. This allows the effective structural health monitoring (SHM) of a wide range of civil-engineering projects facing challenges such as ageing or nearby construction works; key applications include large structures such as bridges, tunnels, railways, power plants and similar utility buildings [2]. By attaching standard optical fibre to any such building or structure, cracks and shifts in the structural body can be discovered quickly and non-invasively [5]. Sensing in this way can increase building safety and allow the construction of increasingly large civil engineering projects, whilst reducing costs and automating previously manual inspection procedures. Competing technologies in SHM such as wireless sensors [6] and visual inspection have drawbacks such as the need for wireless spectrum and battery replacement, and the high costs of maintenance using skilled labour. In contrast, fibre optic sensing requires zero intervention after installation, and can even be embedded within concrete where the internal stress/strain would be invisible to external inspection. Furthermore, the cost of a DFOS system does not generally scale up with sensing distance (in contrast to other solutions), as standard single mode optical fibre is inexpensive.

BOTDA (Brillouin Optical Time Domain Analysis) and COTDR (Coherent Optical Time Domain Reflectometer) systems have already been demonstrated for distributed long-distance sensing [2, 7]. However, there are barriers to achieving dynamic performance using these systems, such as the need to sweep through a large overall frequency span to find the Brillouin frequency shift (or Rayleigh equivalent in the COTDR system); the need for ensemble averaging to increase the Signal-to-Noise Ratio (SNR); and the time taken for the pulse to transit the fibre (in very long-distance sensing) [8]. Novel methods have been developed elsewhere to reduce the time taken for frequency sweeping [9, 10], and this work concentrates on the reduction of ensemble averaging time through careful opto-electronic component selection, intelligent choice of methods for processing the received data and considerations of the ultimate limits to dynamic sensing performance.

Many attempts have been made to model BOTDA and COTDR systems [11, 12]; however these models generally use only the additive white Gaussian noise (AWGN) model applied at the end of pulse transmission simulations. This work seeks to more accurately replicate real-world noise sources, using appropriate probability distributions, and to use the results to suggest optimal components for best performance. There are two major noise contributions within laser sources: phase noise (also known as laser linewidth) and relative intensity noise (RIN). Laser linewidth measures the deviation of the emitted light wave from an ideal sine wave of a specified frequency. RIN measures the deviation of the laser's power from a nominal output optical power (usually the maximum) when held at a constant input power (e.g. constant current for semiconductor diode lasers). These deviations mainly come from spontaneous emission within the laser cavity, a naturally random process. A third noise source in DFOS systems is the thermal and shot noise in detection components. In both the BOTDA and COTDR simulation models, it is assumed that the noise from the photo-detector and any photonic pre-amplification can be specified as the equivalent optical power noise floor of a single AWGN source.

Direct comparison of these two models reveals clear differences. The Rayleigh COTDR system offers very high strain and temperature resolution, but insufficient measurement range for commercial use; the Brillouin BOTDA system has an ideal strain measurement range but is less resistant to noise and requires further averaging to achieve the same SNR as the Rayleigh system.

This paper discusses the barriers to how quickly measurements can be taken, and whether faster measurements would result in a trade-off with measurement quality. Initially the limits imposed by practical equipment capabilities are investigated, to determine the parameters of common equipment setups which result in the highest performance. Towards the conclusion of this paper, mathematical constraints are considered as to the fundamental limits arising from information theory, an interesting area for future work.

II. BOTDA SIMULATION METHODS

Brillouin scattering is an inelastic scattering process, which occurs when light meets an acoustic wave within a medium. Molecules in a solid settle at an equilibrium distance from each other, and oscillate about this central position when perturbed. This motion induces oscillation in neighbouring molecules, and collectively supports the propagation of an acoustic wave through the fibre; when light is incident on this acoustic wave, it can be scattered with a frequency change. The peak frequency shift occurs at a fibre-dependent value, and is of the order of an 11GHz shift for standard silica fibres designed for telecommunications use at 1550nm [13]. This frequency change is sensitive to changes in the properties of the fibre at microscopic scale, with changes in strain and temperature affecting the refractive index and thus changing the local Brillouin frequency shift. By measuring the frequency shift between incident and Brillouin scattered light, the strain and temperature properties of the fibre can be recovered.

The fraction of light that is scattered due to spontaneous Brillouin scattering is small, resulting in a low SNR at the photodetector. To combat this, scattering can be stimulated in order to achieve a higher power of the scattered light. If laser beams are incident from both ends of the fibre, with a frequency difference between them, an acoustic wave is stimulated at the frequency of this frequency difference between the two waves. When this frequency matches the local Brillouin frequency shift, the acoustic wave produces the strongest local Brillouin scattering signals, and the opposing laser beams either gain or lose intensity due to the interactions. By scanning through various laser frequency differences, the intensity of stimulated Brillouin emissions can be measured as a function of frequency shift and the peak frequency shift identified over distance along the fibre.

The local Brillouin frequency shift varies with a linear relationship to temperature and strain:

$$\Delta\nu_B(z) = C_{\nu\varepsilon}\Delta\varepsilon(z) + C_{\nu T}\Delta T(z) \tag{1}$$

where $\Delta\nu_B(z)$ is the change in local Brillouin frequency shift at location z, $\Delta T(z)$ is local temperature (K), $\Delta\varepsilon(z)$ is local strain, and $C_{\nu\varepsilon}$ and $C_{\nu T}$ are constants. These constants are highly fibre dependent, and must be calibrated for each fibre under test [13].

BOTDA systems implement this with a pulsed “pump” laser and a continuous wave “probe” or “Stokes” laser at opposing ends of the fibre, with a frequency offset between them. As this frequency offset is varied, the gain or loss of the pump beam intensity over time is measured.

Through photon time-of-flight calculations, these temporal variations can be related back to distance along the fibre.

The Brillouin system computational model is based on the mathematical derivations from Maxwell equations outlined in depth elsewhere [15, 16] and implemented for a two-laser stimulated Brillouin emission system. A continuous wave probe laser and pulsed pump laser are simulated at opposite ends of a fibre. A steady state solution is found for the power of the pump and probe laser propagation through the fibre, before the application of a novel equation derived from the three wave mixing equations to find the Brillouin gain for each frequency difference (ω) between pump and probe lasers [15]:

$$G(z,\omega) = E_s^{CW}(z)\left(\mathbf{E_p}(0,\omega) \otimes \frac{\mathbf{E_p}(0,\omega)}{\Gamma_1 - j(\Delta(z)+\omega)}\right) \tag{2}$$

where $G(z,\omega)$ is Brillouin gain, $E_s^{CW}(z)$ the Stokes laser amplitude and $\mathbf{E_p}(0,\omega)$ the probe laser amplitude, with other constants as derived in [15]. This process is then repeated whilst the frequency difference between pump and probe lasers is varied in steps across the whole range.

The raw data has the constant background Brillouin scatter level subtracted, which otherwise forms a "DC offset" to the scatter signal which varies through the fibre. A Lorentzian fitting scheme is applied across the frequency span using cross-correlation [17], before converting the frequency shift at the fitted peaks to strain values using the empirical formula in equation (1).

To model laser linewidth, a Lorentzian model is used [18]. This is implemented via the ratio of two Gaussian distributions applied to the frequency of the laser source. To model the laser RIN, it is assumed that the laser power fluctuates at the source with a Gaussian profile. A percentage value can be specified (as generally given by laser diode manufacturers), and this can be converted to the width of Gaussian required for accurate modelling. To model detector noise, a white Gaussian noise floor (converted to an optical power equivalent) is specified at the detector; this value incorporates the noise from any additional optical or electrical pre-amplification.

Further assumptions made in the model include a lack of polarisation sensitivity (achievable in practice through use of a polarisation scrambler with ensemble averaging); no amplification in the

fibre and thus no optical noise generated along the length of the fibre; and linear attenuation (due to Rayleigh scattering and absorption) through the fibre, with no splicing losses.

Throughout this work, the SNR for each system has been calculated as follows: the mean difference between the optical signal power as measured by the detector including the specified noise types, and the optical power measured for a simulated ideal case with zero noise has been calculated, with power measurements filtered to a 0.1nm/12GHz bandwidth. The ratio of this power difference and the mean signal power was taken and then averaged across all frequencies within the sweeping for a given set of components. No averaging was applied unless stated.

III. COTDR SIMULATION METHODS

Rayleigh scattering differs from Brillouin scattering in that it is a fully elastic process, meaning that no frequency change is observed in the scattered light. The scattering originates from the shifting of the electron clouds of the atoms and molecules of the fibre in response to the applied electric field - the sinusoidal laser field causes the electron cloud to locally oscillate in phase with it, resulting in light emission in all directions from the scattering centre. A fraction of the light is scattered in the exact opposite direction to the incident light, and which is retained within the waveguide structure of the fibre and guided back to the source. The electric fields from each scattering centre can be assumed to sum linearly to give an overall response within the laser pulse time, and the received power will thus depend on both amplitude and phase of each reflection within the pulse length.

The computational model considers the fibre to be split into a large number of small sections [11, 12, 20]. The end of each section behaves as if it were a small mirror, at which a varying proportion of the laser light (incident from only one end of the fibre) is reflected with a phase change. The total backscattered power $P(z)$ can then be calculated [11]:

$$
\begin{aligned}
P(z) &= |E(z)|^2 \\
&= \left[\sum_{i=1}^{M} a_i \exp(j\Omega_i)\right]\left[\sum_{i=1}^{M} a_i \exp(-j\Omega_i)\right] \\
&= \sum_{m=1}^{M}\sum_{n=1}^{M} a_m a_n \exp\left[j(\Omega_m - \Omega_n)\right]
\end{aligned}
\tag{3}
$$

Where $E(z)$ is the complex amplitude of backscatter signal at distance *z* along the fibre, *M* is the total number of scatterers in the scattering region, a_i and Ω_i are the amplitude and phase response at each mirror *i* respectively, with renumbering to *m* and *n* for mathematical simplicity.

The phase change between two successive scattering centres can be notated as

$$\Omega_m - \Omega_n = 4\pi f_0 \Delta L_m n_0 / c \tag{4}$$

where f_0 represents the frequency of light, ΔL_{mn} is the space distance between *m*th and *n*th scattering centres , n_0 is the refractive index, and c is the vacuum velocity of light.

It is noted that Rayleigh scattering in a homogeneous medium would result in the scattered light returning in phase, but the local variant electromagnetic environment of atoms in solids and liquids results in non-uniform phase changes. The key to this method relies on the invariance of those Rayleigh scattering properties over time - the scattering pattern along a fibre effectively creates a “fingerprint” response to applied laser light along its length, and each fibre will always give the same phase and amplitude response. In an ideal world the size of each scattering centre in the model would be set at the same order of the wavelength of light to match the physical principles behind the scattering, however given the linearity of the superposition of each scattering centre's contribution, the computation can be performed for a larger step-size to reduce computation time without loss of generality [11].

The Rayleigh response of the fibre is assumed to be constant over time without any external influences. However, the phase changes depend on both incident frequency and refractive index. Changes in strain or temperature can change the local refractive index, but this effect can be “cancelled out” by a laser frequency change [11]. The frequency shift that gives the same phase

change and thus backscatter pattern as any strain/temperature perturbed section can be found using a cross-correlation technique between the perturbed and unperturbed cases [12]. The fibre strain can then be recovered using an empirical formula given in [19].

All assumptions regarding noise modelling, polarisation and optical unit standardisation as discussed in section II for the BOTDA system remain identical for the COTDR system.

IV. RESULTS – GENERAL OBSERVATIONS

a. Variable ensemble averaging limits

Ensemble averaging of raw data from DFOS systems can enhance the final SNR, however the enhancement can reach a limit for any given system. Figure 1 shows an example for BOTDA systems of various SNRs before averaging. These simulations considered the Time Domain Spatial Resolution (TDSR), defined as the distance equivalent of the 10-90% rise time of strain data for a step change in strain in the simulated fibre. Although the pulse width provides a fundamental limit to spatial resolution, a poor system SNR will increase this limit. A smaller TDSR therefore corresponds to a larger SNR. Figure 1 also indicates that systems of various SNRs all converge to the same limit, and further averaging after reaching that point provides no overall benefit to the final results of the system – a steady state of best performance.

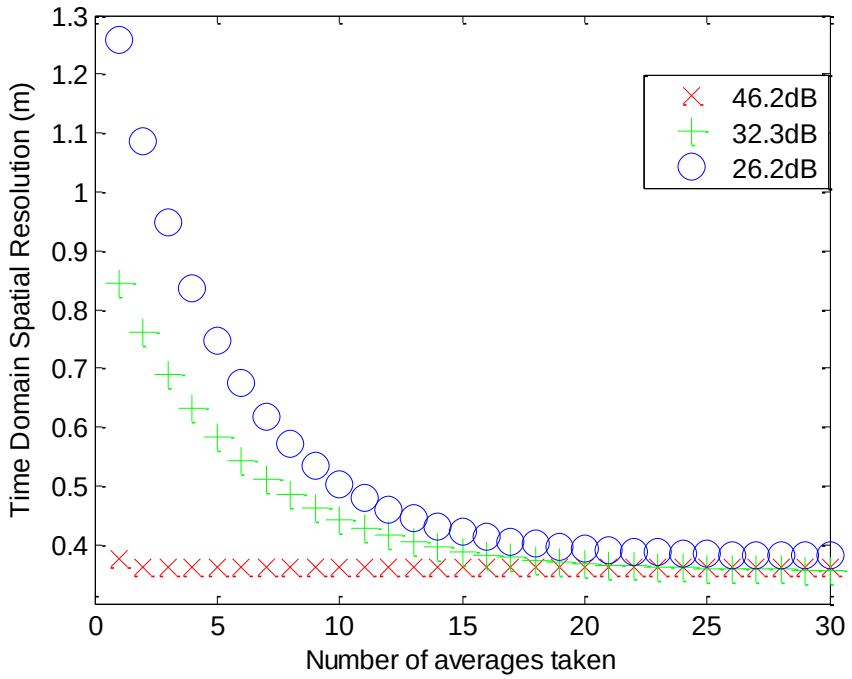

Figure 1: Time domain spatial resolution after ensemble averaging for BOTDA systems of various SNRs – SNRs quoted before averaging.

b. Ensemble averaging position within signal processing

The signal processing described in sections II and III above is shown as a flow chart for each system in figure 2. The averaging technique could be applied at any stage of the signal processing, however table 1 shows the SNR achieved after 200 averages for both systems dependent on the sequence in the workflow.

It is shown in table 1 that the earlier in the signal flow that averaging is performed, the better the final SNR. Thus the averaging should be performed on raw data at the photo-detector to minimise averages required (and thus time taken) to enhance SNR.

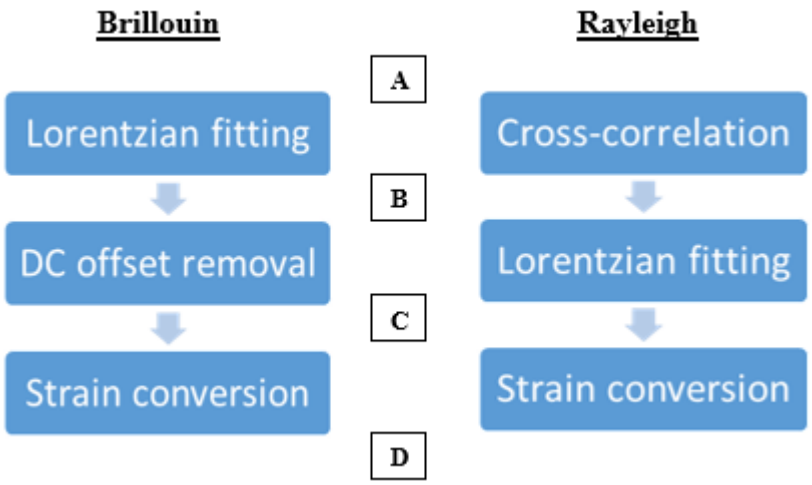

Figure 2: The signal processing flows for both BOTDA and Rayleigh COTDR systems, as derived in sections II and III.

DSP Position	Brillouin SNR (dB)	Rayleigh SNR (dB)
A	24.1	4.98
B	22.0	4.20
C	20.3	3.83
D	20.3	3.83

Table 1: SNR at various stages of signal processing, at points shown in figure 5, after 200 averages, assuming 1MHz linewidth, -40dBm detector noise floor and 3% RIN.

V. NOISE ANALYSIS – BOTDA SYSTEM

a. Brillouin System Parameters

For BOTDA, a frequency sweep step of 5MHz over a 200MHz range was used to gather data on a 50m fibre with a 10με strain perturbation across 1m at its centre. It is also assumed for this BOTDA simulation that laser noise sources apply identically to both pump and probe lasers.

b. Laser Linewidth

Figure 3 shows the change in SNR as the laser linewidth is varied, at constant 3% RIN and -40dBm detector noise floor. The flat region below 0.1MHz demonstrates that below that turning point, other noise sources dominate rather than the laser linewidth. Each laser pulse emitted is considered to be identical, with the same total energy, and when this energy is spread over a broader range of the spectrum due to a larger linewidth, the energy of the signal at the desired frequency will be weaker. To maintain a high SNR whilst utilizing only low cost components and thus the least averaging times and faster signal processing, a laser linewidth of 0.1MHz is recommended for a BOTDA system.

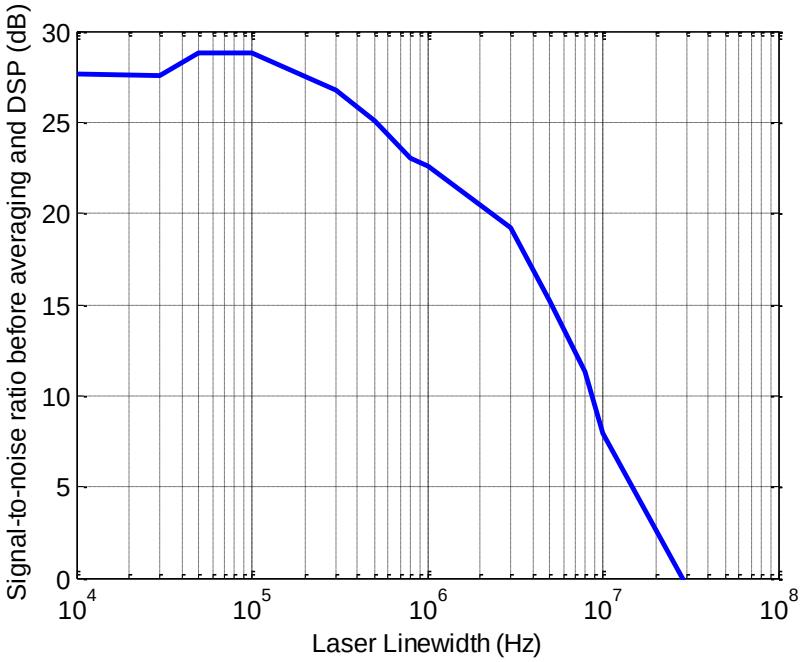

Figure 3: SNR as a function of laser linewidth for a BOTDA system.

c. Laser Relative Intensity Noise

Figure 4 shows the change in SNR as the laser RIN is varied, at 40dBm detector noise floor and constant 1MHz linewidth. There is far less variation of SNR with RIN as with other noise sources, because the RIN causes small perturbations to intensity without affecting the frequency. Therefore, the overall Brillouin frequency response is reasonably well preserved.

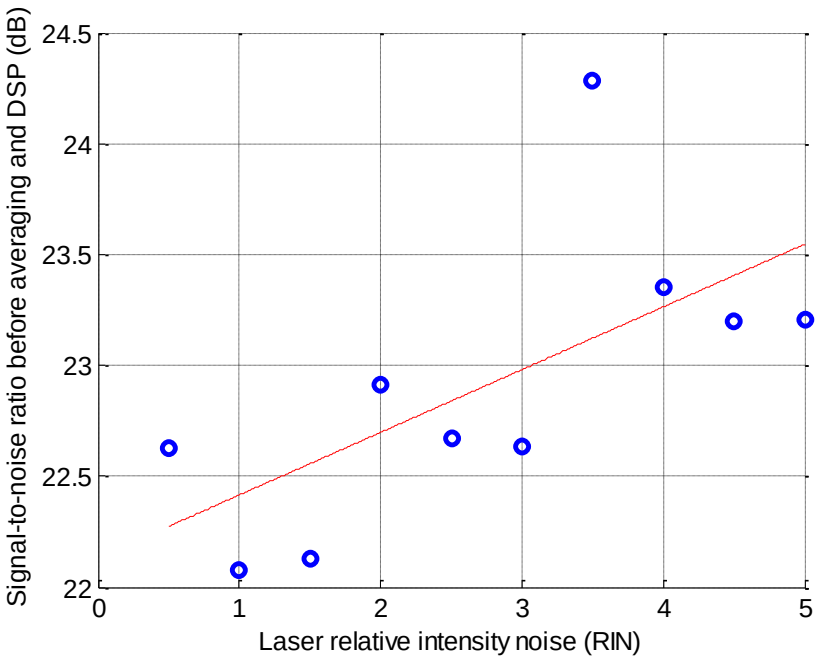

Figure 4: SNR as a function of laser RIN (%) for a BOTDA system.

Since the RIN distribution is assumed to be Gaussian on both pump and probe laser sources, on average the RIN could cancel out due to opposing positive and negative intensity fluctuations on each laser, that effectively removes any overall power variation within the fibre when both pump and probe contributions are summed. For instance, a simultaneous increase in pump power and decrease in probe power gives the same total instantaneous power within the fibre – statistically this should occur for 50% of samples due to the Gaussian distribution of RIN.

d. Receiver/Detector Noise

Figure 5 shows the change in SNR as the noise floor of the detector is varied, with constant 1MHz laser linewidth and 3% RIN. The linearly increasing section demonstrates the dominance of thermal and shot noises at the detector over all other noise sources for a noise floor of -40dBm or greater, whilst the flat region for noise floors <-40dBm implies that other noise sources are now becoming

the governing factor. For this BOTDA system, if seeking high SNR to minimise averaging time, there would be no benefit to use an expensive low noise floor detector below -40dBm without improving other components.

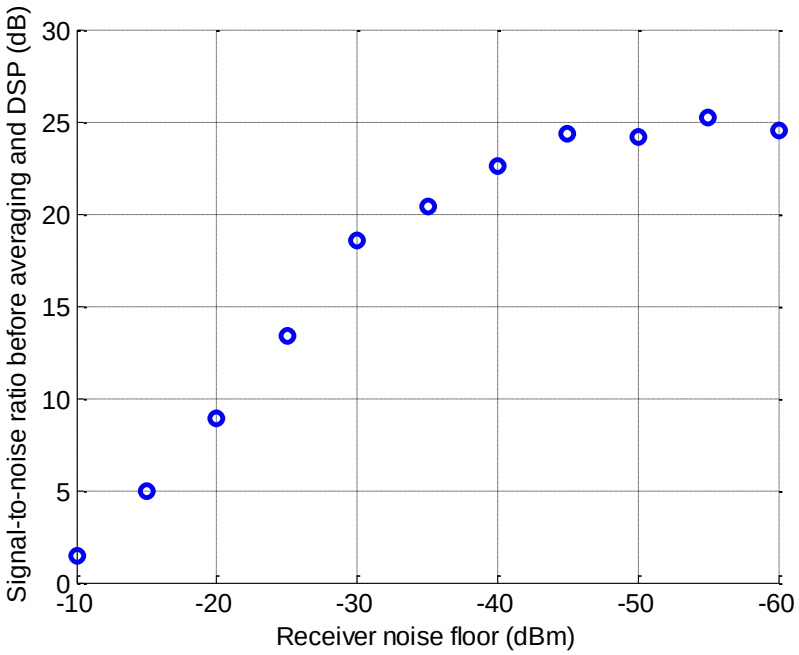

Figure 5: SNR for varied receiver noise floor in equivalent optical power (dBm) in a BOTDA system

VI. NOISE ANALYSIS - RAYLEIGH COTDR

a. System Parameters

For COTDR, a frequency sweep step of 5MHz over a 200MHz range was used to gather data on a 50m fibre with a $1\mu\varepsilon$ strain perturbation across $1m$ at its centre. A smaller strain perturbation was used for Rayleigh COTDR than that of BOTDA in section 3.2 due to its better achievable resolution, else a substantially greater frequency sweep size would have been required [15].

b. Laser Linewidth

Figure 6 shows the change in SNR as the laser linewidth is varied, at constant 3% RIN and -40dBm detector noise floor. Similarly to the BOTDA system, a limit is found below which linewidth is no longer the dominant noise source, however this limit is now 10MHz. Despite most coherent optical systems relying on low phase noise, COTDR has been shown here to have greater linewidth tolerance than BOTDA. In practical systems and in this simulation, the scattering centres are spaced closer together than the spatial length of the pulse. This means that single pulses contain contributions from multiple scattering locations. Thus this system displays a level of inherent averaging, as the linewidth can effectively average out over the entire pulse length. However for large linewidths (10MHz or more) this effect is less prominent, due to the small number of scattering centres simulated within each pulse duration in this system.

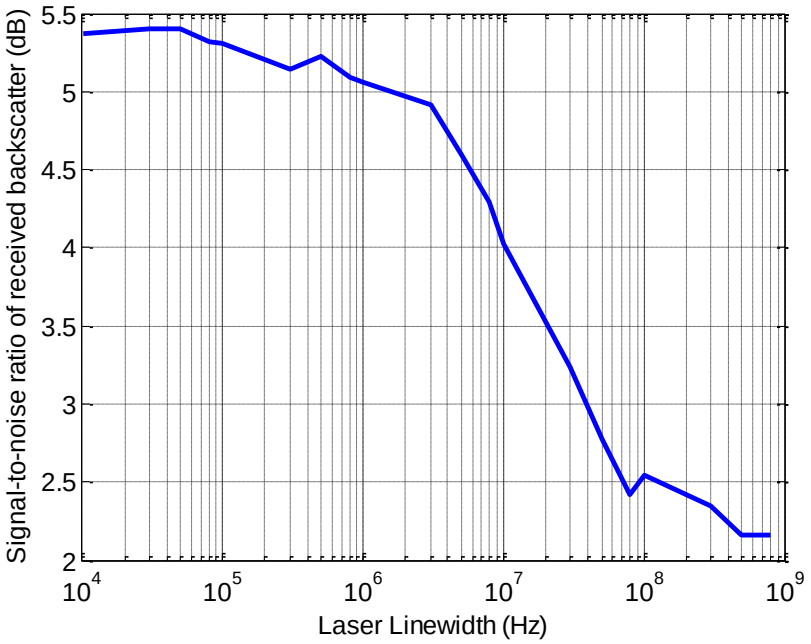

Figure 6: SNR for varied laser linewidth in a COTDR system

c. Laser Relative Intensity Noise (RIN)

Figure 7 shows the change in SNR as the laser RIN is varied, at constant 1MHz linewidth and -40dBm detector noise floor. As with the BOTDA system, the variation of SNR is low, <0.5dB over the 0-5% range studied, for the same reasons as given in section 3.2.2. This value refers to the optical signal at the detector only, but the cross-correlation step of the DSP which follows the detection is also highly resistant to small changes in instantaneous intensity [21], searching only for localised matches in intensity pattern over a patch, thus showing even further tolerance of RIN.

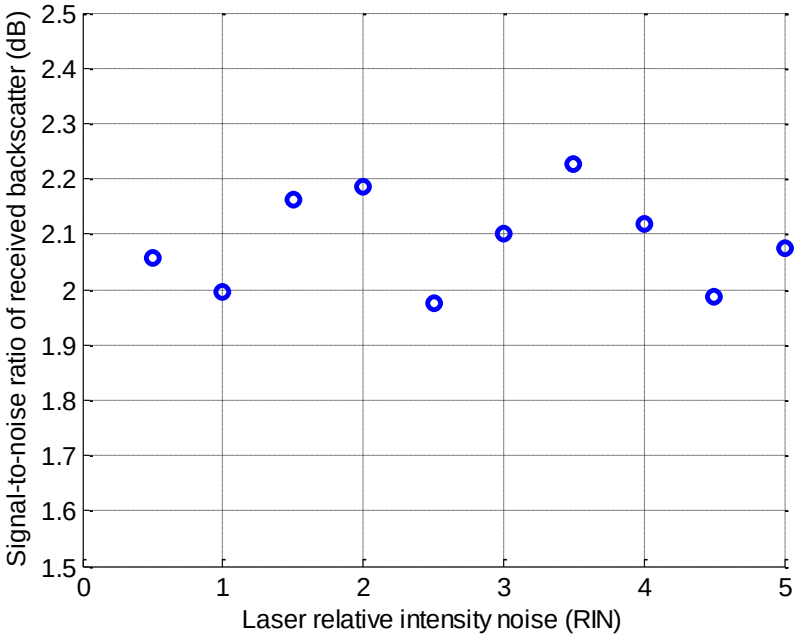

Figure 7: SNR for varied laser RIN in a COTDR system

d. Receiver/Detector Noise

Figure 8 shows the change in SNR as the detector noise floor is varied, at constant 1MHz linewidth and 3% RIN. As with the BOTDA system there is a linear relation between the receiver noise floor and overall SNR, up until a point (here -60dBm) where the noise floor is no longer the noise source of greatest prominence.

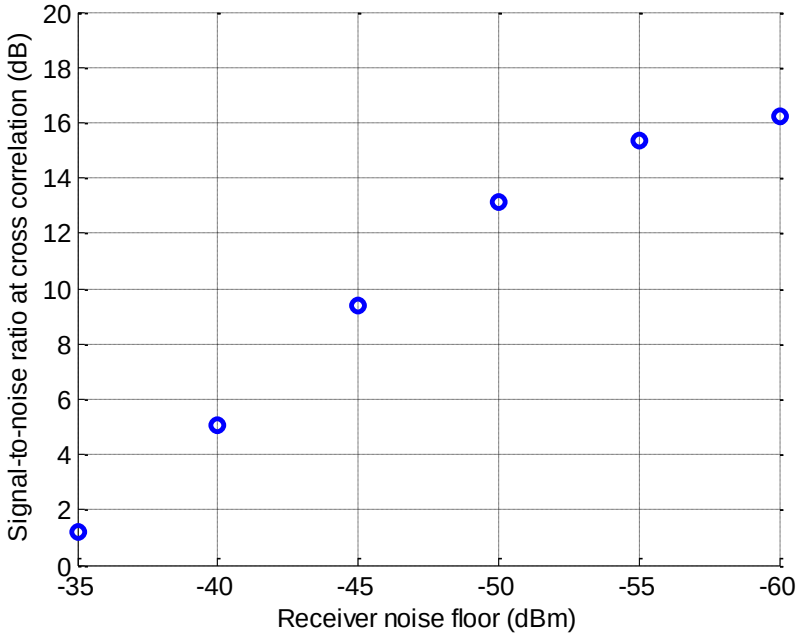

Figure 8: SNR for varied receiver noise floor in equivalent optical power (dBm) in a COTDR system

VII. COMPARISON BETWEEN BOTDA AND COTDR

a. Dynamic strain sensing range

The coefficients relating Brillouin frequency shift to strain and/or temperature (equation 1) only hold for a Brillouin system and set the scale over which the sensor operates. However, for comparison with a COTDR system as simulated here, a second set of coefficients are found to relate the Rayleigh frequency "shift" to the strain and temperature of the fibre. For the Brillouin system, a Brillouin frequency shift of 1MHz corresponds to a strain change of $20\mu\varepsilon$ (from empirical formulae taken from an average of a wide range of fibres [14]). For the Rayleigh system, a

frequency shift of 1MHz corresponds to a strain change of 0.0066$\mu\varepsilon$ (again, an average across several fibres [11]).

To meet industrial requirements, a range of strain detection from 1$\mu\varepsilon$ to 10000$\mu\varepsilon$ (or equivalently 1% strain) is the optimum range for a commercial product. To achieve this, the Rayleigh COTDR system would require a tuning range of 151GHz, a difficult requirement for a single laser. Although a DFB/DBR/VCSEL laser may state a maximum tuning range of up to 4nm, corresponding to 499GHz, it is unlikely that performance characteristics would remain constant over this range; non-linearities or imperfections would be expected to distort the measurements. Even if possible, tuning across such wide frequency steps will also take longer time to settle and will result in noisier transitions between frequencies, reducing the practicality of dynamic sensing.

A secondary issue relates to the need for more intelligent processing algorithms for the COTDR system, given the nature of phase variation. Phase changes are periodic around 2π and as such the detected frequency pattern also displays periodicity. If the sweep through frequency steps relates to a phase change variation of greater than 2π, the observed cross-correlation pattern would spread across several bands of phase - choosing the correct result at a given perturbation in modulus 2π arithmetic is non-trivial. Slight deviations occur between each correlation due to the noise, so an advanced algorithm will be required to ensure that the correct band is selected for the final result.

For the ultimate performance resolution, the COTDR method could be enhanced even further through the use of an alternative laser central wavelength. By decreasing the wavelength to the next nearest low loss band in standard optical fibre at 1.3μm, the frequency shift is reduced even further still, to 5.9$n\varepsilon$. This does incur a slight increase in the power loss per unit distance, so would not be recommended for long spans, but could provide even greater precision if required.

Unless solutions are found to both issues with the COTDR system, the reduced strain measurement range would not be acceptable for practical use, and a BOTDA system would be a better solution.

b. Accuracy over distance

The measurement uncertainty for the Brillouin system is noted to increase with the distance from the detector at which the measurement is performed. The simplest explanation for this is the increase in SNR along the length of the fibre, simply due to the amount of loss experienced [22]. However, the Rayleigh system suffers differently due to the same effect. This is due to a key misleading name in the Rayleigh based system. Although it could be assumed that a coherent system would deteriorate after the coherence length of the source has been exceeded, the coherence effect used here is only over the length of the pulse used. For a 10ns or less pulses, all true laser sources should be able to produce a coherent beam.

The Brillouin data is based upon absolute measurements of intensity in order to infer the frequency response across the whole sweep, so it is far more important that the intensity values at their return to the detector are accurate and as large as possible. In comparison, the Rayleigh data processing relies on cross-correlation between the perturbed and unperturbed cases. In theory, both cases will experience the same loss over distance and the cross-correlation should remain unaffected. Due to the noise present in the system this is not the case, but the Rayleigh system is more robust and tolerant in the presence of noise.

This simulation work is backed up by experimental findings elsewhere [22], although quantisation of the effect has not yet been possible and is left for future work.

c. Suitability for dynamic sensing

With all of the information from the preceding sections now available, it is clear that the two candidate systems are not directly comparable. Although the Rayleigh COTDR system requires less averaging in order to secure a higher SNR, the lack of sufficient measurement range is a big drawback. Therefore the increase in acquisition speed would not be an acceptable trade-off in a commercial system which requires a larger measurement range. The BOTDA system shows promising dynamic ability, particularly if more intelligent algorithms are found to fit smaller frequency shifts. If care is also taken to reduce the number of ensemble averages required by

observing the performance limits beyond which further averaging is futile, the measurement acquisition time can be further decreased.

VIII. THEORETICAL FUNDAMENTAL LIMITS

All results found above rely on the properties of the equipment used to perform the sensing. Even though progress in photonic systems may currently limit the achievable sensing resolutions, if practicality was no barrier there may be fundamental limits imposed on the achievable results.

A cornerstone of information theory holds that for any information carrying channel, a fundamental upper bound exists to the rate at which information can be carried by the channel. The implications for fibre sensors include the fact that the fibre both senses and carries information - it is important to separate out the stages of sensing and encoding the information and the subsequent transfer of that information from the remote sensing locations to the receiver. It is thus difficult to quantify the information content in terms appropriate for analysis by information theoretic principles.

For instance, the most often quoted theorem from information theory concerns the information carrying capacity that a channel is ultimately capable of. The Shannon-Hartley capacity theorem states:

$$C = B\log_2\left(1+SNR\right) \tag{5}$$

for channel capacity (bits/second) *C*, and bandwidth of signal *B* [23]. This assumes a channel of additive white Gaussian noise, a reasonable approximation to the fibre sensing systems discussed. The impact on this search for the limits to dynamic sensing concern the bandwidth of the signal, and the received SNR.

This approach is not as simple as it first appears. Although the channel capacity final result is given in terms of a bits-per-second value, it would be completely incorrect to assume that corresponds to the maximum possible product of digital bit-depth and sampling rate. The channel capacity provides an absolute upper bound to the possible data rate, which in general can only be realised using an advanced coding scheme. This scheme is not specified, but Shannon's work merely proves

that such a scheme exists. Moreover, the information content of a signal also relies upon the relative probabilities and entropy of the symbol set chosen on which to encode the data. In this case, the data can always be considered a frequency modulated signal of the carrying laser light. Although pulse coding techniques may be able to increase SNR, they do not affect the base encoding method of the data concerned (strain and temperature information) onto the light through frequency modulation - the natural process occurring in the fibre.

Therefore, the relevance of this concept to the ability of a sensor to provide information at a fast rate is not obvious or linear, and cannot at this stage be quantified. It is expected that the theoretical limit to information transfer of this type will not be reached in the near to mid-future, and that this type of analysis is not currently fruitful for developing dynamic sensing products.

IX. CONCLUSIONS

Both BOTDA and Rayleigh COTDR fibre optic sensing systems have shown great promise in structural health monitoring, but require long data acquisition time to improve SNRs by numerous ensemble averages. A noise model has been built to analyse the contributions of multiple noise sources in both DFOS systems. Laser linewidth and receiver thermal/shot noise are found to be more dominant over laser relative intensity noise for both BOTDA and Rayleigh COTDR systems. Reducing laser linewidth is more important in a BOTDA than a Rayleigh COTDR system.

Ensemble averaging only improves SNR to a certain limit in any given system; the number of ensemble averages required could be varied according to prevailing system parameters. An algorithm could be found to measure the properties of the DFOS system and adjust averaging to increase measurement speed, working towards dynamic sensing. With appropriate choice of components, higher SNRs can be achieved with less averaging, leading to faster data acquisition for dynamic sensing.

Analysis of both systems as if they used the same optical components and parameters does not give a clear preferred sensing method. Rayleigh COTDR has much better strain resolution, but insufficient strain range; BOTDA has an ideal strain range but requires additional ensemble

averaging for robustness to noise. Once both of the above issues are solved, both BOTDA and Rayleigh COTDR systems would show promise for dynamic sensing for real time applications.

X. ACKNOWLEDGEMENTS

This project was carried out under the UCL-Cambridge Centre for Doctoral Training in Photonic Systems Development, with funding from EPSRC (EP/G037256/1) gratefully acknowledged. The support from the Cambridge Centre for Smart Infrastructure and Construction is also acknowledged. Special acknowledgement to Prof Aldo Minardo for his profound advice and discussion on the BOTDA model.

XI. OPEN DATA STATEMENT

Additional and supporting data will be accessible at http://www.repository.cam.ac.uk/handle/1810/248986

XII. REFERENCES

[1] Bao X. and Chen L., “Recent Progress in Distributed Fiber Optic Sensors”, Sensors, 12: 8601:8639, 2012.

[2] Glisic B., “Distributed Fiber Optic Sensing Technologies and Applications – An Overview”, American Concrete Institute Special Publication, 292: 1-18, 2013.

[3] Qin Z, Zhu T. and Bao X., "High frequency response distributed vibration sensor based on all polarization-maintaining configurations of phase-otdr", IEEE Photonics Technology Letters, 23: 1091-1093, 2011.

[4] Qin Z., Chen L. and Bao X., "Wavelet denoising method for improving detection performance of distributed vibration sensor", IEEE Photonics Technology Letters, 24: 542-544, 2012.

[5] Ravet F., Briffod F., Glisic B., Niklès M., and Inaudi D., "Submillimeter Crack Detection With Brillouin-Based Fiber-Optic Sensors", IEEE Sensors Journal, vol 9, 11:1391-1396, 2009.

[6] Hughes J., Yan J. and Soga K., "Development of wireless sensor network using bluetooth low energy (BLE) for construction noise monitoring", International Journal on Smart Sensing and Intelligent Systems, vol. 8, 2:1379-1405, 2015.

[7] Palmieri L. and Schenato L., "Distributed Optical Fiber Sensing Based on Rayleigh Scattering", The Open Optics Journal, 7: 104:1274, 2013.

[8] Peled Y., Motil A., Yaron L. and Tur M., "Fast and distributed Brillouin time domain analysis of optical fibers", Proc. SPIE, 8421:842113 OFS2012 22nd International Conference on Optical Fiber Sensors, 2012.

[9] Bernini R., Minardo A. and Zeni L., "Dynamic strain measurement in optical fibers by stimulated brillouin scattering", Optics Letters, 34: 2613-2615, 2009.

[10] Taki M., Muanenda Y., Oton C. J., Nannipieri T., Signorini A. and Di Pasquale F., "Cyclic pulse coding for fast botda fiber sensors", Optics Letters, 38: 2877-2880, 2013.

[11] Zhi Y., Pengxiang S. and Yongqian L., "Research on cotdr for measuring distributed temperature and strain", 2011 Second International Conference on Mechanic Automation and Control Engineering (MACE):590-593, 2011.

[12] Yongqian L., Rongwei L. and Zhi Y., "Coherent otdr for measuring distributed temperature and strain with high resolution in km-long fiber", 2010 International Conference on Intelligent Computation Technology and Automation, 1:962-965 2010.

[13] Shiraki K., Ohashi M., and Tateda M., "SBS Threshold of a Fiber with a Brillouin Frequency Shift Distribution", Journal of Lightwave Technology, 14:50-57, 1996.

[14] Peled Y., Motil A., Kressel I. and Tur M., "Monitoring the propagation of mechanical waves using an optical fiber distributed and dynamic strain sensor based on BOTDA", Optics Express 21 (2013), pp. 10697-10705.

[15] Minardo A., Bernini R. and Zeni L., "Stimulated brillouin scattering modelling for high-resolution, time-domain distributed sensing", Optics Express, 15: 10397-10407, 2007.

[16] Minardo A., Bernini R. and Zeni L., "Numerical analysis of single pulse and differential pulse-width pair botda systems in the high spatial resolution regime", Optics Express, 19: 19233-19244, 2011.

[17] Farahani M.A., Castillo-Guerra E. and Colpitts B.G., "A Detailed Evaluation of the Correlation-Based Method Used for Estimation of the Brillouin Frequency Shift in BOTDA Sensors", IEEE Sensors Journal, 12: 4589:4598, 2013.

[18] Henry C.H., "Theory of the linewidth of semiconductor lasers", IEEE Journal of Quantum Electronics, 18: 259-264, 1982.

[19] Li W., Bao X., Li Y. and Chen L., "Differential pulse-width pair botda for high spatial resolution sensing", Optics Express, 16:21616-21625, 2008.

[20] Shimano R., Iitsuka Y., Kubota K. and Koyamada Y., "31-km distributed temperature measurement with very high resolution using coherent-otdr enhanced with bidirectional edfa", 15th OptoElectronics and Communications Conference (OECC2010) Technical Digest, 330-331, 2010.

[21] Koyamada Y., Imahama M., Kubota K. and Hogari K., "Fiber-Optic Distributed Strain and Temperature Sensing With Very High Measurand Resolution Over Long Range Using Coherent OTDR", Journal of Lightwave Technology, 27: 1142-1146, 2009.

[22] Delepine-Lesoille S., Guzik A., Bertrand J., Henault J-M., and Kishidab K., "Validation of TW-COTDR method for 25 km distributed optical fiber sensing", Proc. SPIE 8794:879438 Fifth European Workshop on Optical Fibre Sensors, 2013.

[23] Shannon C. E., "Communication in the Presence of Noise", Proceedings of the IRE vol. 37, 1:10-21, 1949.